A Moonlighting Role for SPCA2 in E-cadherin Biogenesis and Suppression of Epithelial-Mesenchymal Transition

Donna K. Dang[1], José P. Llongueras[1], Hari Prasad, Isaac Ogunmola, Monish Ram Makena and Rajini Rao[2]

Department of Physiology, The Johns Hopkins University School of Medicine, 725 N. Wolfe Street, Baltimore MD 21205

[1]Co-First Authors

[2]Correspondence: Rajini Rao, Ph.D.

Phone: 410 955 4732

Email: rrao@jhmi.edu

Twitter: @madamscientist

Running Title: Pump-independent role of SPCA2 in E-cadherin biogenesis

Summary

Progression of benign tumors to invasive, metastatic cancer requires loss of the cell-adhesion protein E-cadherin. Although intensive efforts have focused on gene repression and silencing mutations, much less is known about posttranslational control of E-cadherin expression in cancer. SPCA2 is a secretory pathway Ca^{2+}-ATPase that is down-regulated in metastatic breast cancer. We show that SPCA2 is tightly co-expressed with epithelial signature genes and required for E-cadherin biogenesis and cell surface expression. Unexpectedly, this function is uncoupled from Ca^{2+} pumping and mediated by binding to E-cadherin. Loss of SPCA2 is sufficient to disrupt cell-cell adhesion in tumorspheres and elicit mesenchymal gene expression through Hippo-YAP signaling. These findings point to a causal link between low SPCA2 levels and the epithelial-mesenchymal transition required for breast cancer metastasis.

Keywords: *ATP2C2*, epithelial-mesenchymal transition, E-cadherin

Highlights

- SPCA2 is an epithelial marker transcriptionally linked to E-cadherin expression
- Loss of SPCA2 impairs E-cadherin biogenesis independent of Ca^{2+} pump activity
- SPCA2 is required for tumorsphere formation and Hippo-YAP signaling to antagonize epithelial-mesenchymal transition
- Down-regulation of SPCA2 in metastatic cancers may contribute to malignancy

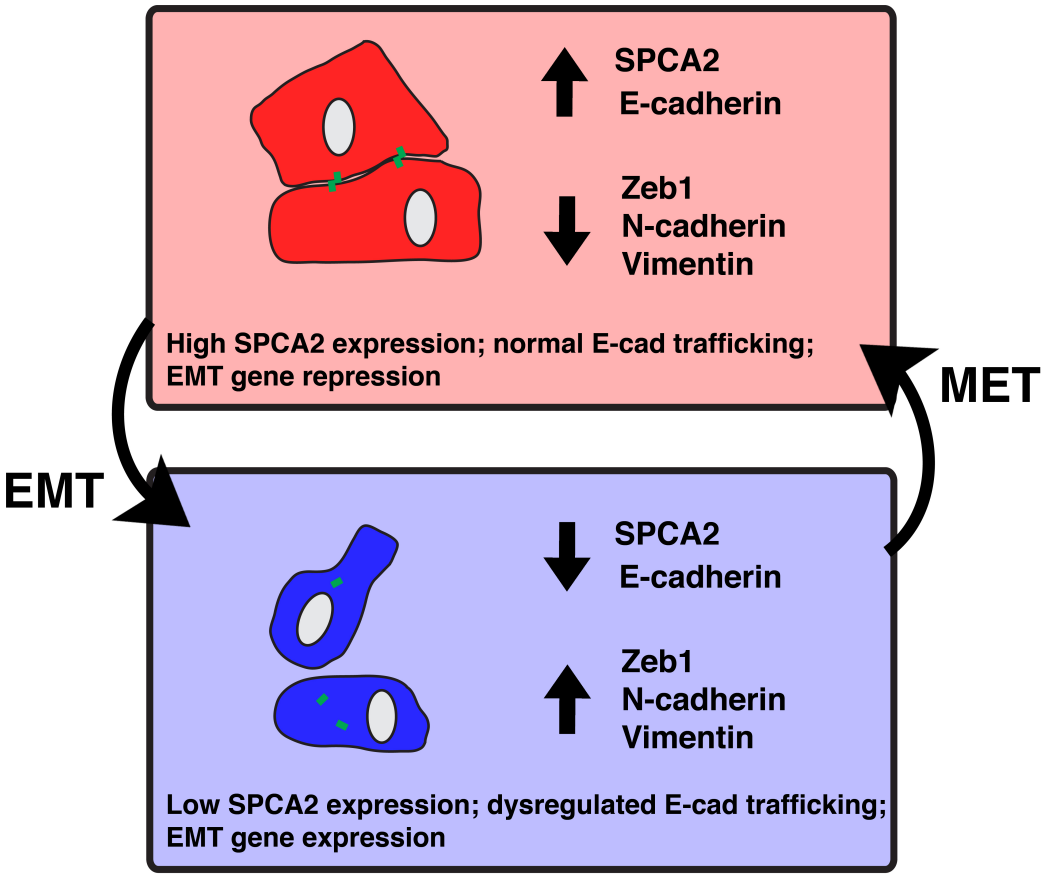

Introduction

Mortality from breast cancer is invariably due to tumor metastasis, which requires a key step known as epithelial to mesenchymal transition (EMT) during which cancer cells lose their polarity and cell-cell contacts, thereby acquiring the ability to migrate (1, 2). The process of EMT coincides with the loss of epithelial markers; the most critical of these is the Ca^{2+} binding cell adhesion protein E-cadherin. Progression of benign tumors to invasive, metastatic cancer requires the loss of E-cadherin (3). As a structural component of the adherens junction in polarized epithelial cells, E-cadherin is a membrane-spanning protein that mediates homophilic cell-cell contacts through its extracellular domains and communicates these interactions via its intracellular domains to a network of signaling proteins to control cell polarity, organ size and epithelial integrity (4-6). Thus, contact inhibition of growth is transmitted by E-cadherin to the Hippo signaling pathway, resulting in nuclear exclusion and inactivation of the transcriptional co-activator YAP (Yes-activated protein) and its paralog, TAZ (transcriptional activator with PDZ binding motif) (5, 7). Loss of Hippo signaling or overexpression of YAP/TAZ promotes metastatic phenotypes, including EMT (8). Furthermore, EMT correlates with the generation of cancer stem cells and multidrug resistance. A better understanding of the molecular pathways that down-regulate E-cadherin and control the Hippo pathway may be pivotal to discovering new therapeutic targets for treatment of metastatic cancers.

E-cadherin expression is regulated at multiple levels, including genetic, epigenetic, transcriptional and post-translational. At the transcriptional level, *CDH1*, the gene

encoding E-cadherin is repressed by a set of nuclear factors, including ZEB1 and SNAI2/SLUG that reprogram the cancer cell to acquire malignant invasive phenotypes (9). Expression of these factors in breast cancer tissue inversely correlates with E-cadherin and prognosticates a more aggressive, invasive phenotype with poor clinical prognosis. In contrast to the wealth of information on *CDH1* regulation, much less is known of oncogenic control of E-cadherin biogenesis despite evidence that post-translational down-regulation of E-cadherin precedes repression of transcription upon induction of EMT (10).

In this study, we describe a non-canonical, isoform-specific interaction between E-cadherin and SPCA2, one of two secretory pathway Ca^{2+}-ATPases that transports Ca^{2+} ions into the Golgi lumen for protein sorting and quality control. Although they have similar ion transport characteristics and appear redundant at first glance, we show that SPCA2, but not SPCA1, is an epithelial signature gene required for biogenesis of E-cadherin, maintenance of cell adhesion and contact inhibition of EMT. Remarkably, these functions are independent of the Ca^{2+} pumping role of SPCA2 and appear to be mediated by direct protein interaction. By acting upstream of the Hippo pathway, SPCA2 maintains nuclear exclusion of YAP and transcriptional repression of EMT genes. This transport-independent moonlighting function of SPCA2 as a selective protein chaperone has implications for cancer evolution.

Results

SPCA2 is an epithelial marker tightly linked to E-cadherin expression

Gene expression correlations offer unique insight on disease pathophysiology, based on the premise that genes expressed together are likely to function together in a pathway (11, 12). Both SPCA isoforms have previously been implicated in breast cancer oncogenesis (13-15). To distinguish between their functions, we compared the expression of SPCA1 (*ATP2C1*) and SPCA2 (*ATP2C2*) genes in breast cancer patient specimens from TCGA (n=526) with a "benchmark" gene set, consisting of 18 epithelial signature genes (ESG) and 13 mesenchymal signature genes (MSG), described previously (11). As expected, we observed a sharp dichotomy between ESG and MSG, with the epithelial and mesenchymal genes separating as two tightly distinct and mutually correlated clusters (Fig. 1A). SPCA1 and SPCA2 showed differential clustering with MSG and ESG, respectively, despite their high identity (64%) in amino acid sequence and similar Ca^{2+} transport characteristics (16, 17). Unexpectedly, we observed a strong correlation between SPCA2 and E-cadherin (Fig. 1A; Fig. S1C Pearson coefficient 0.44; $p = 2.52 \times 10^{-26}$). *CDH1* and *ATP2C2* are both located on the long arm of chromosome 16, whereas *ATP2C1* is on chromosome 3 (Fig. S1A). Consequently, copy number variations of SPCA2 and E-cadherin are tightly linked (Fig. S1B; Pearson coefficient 0.81; $p = 9.99 \times 10^{-124}$). In this context, we note that copy number variations at chromosome 16q lead directly to global deregulation of gene expression implicated in breast cancer

tumorigenesis (18, 19). In contrast, there was no significant correlation, either in copy number variation or mRNA, between SPCA1 and E-cadherin expression (Fig. S1D-E).

To corroborate these findings, we evaluated SPCA gene expression in breast cancer cell lines of the Broad Institute's Cancer Cell Line Encyclopedia (CCLE), previously classified into epithelial and mesenchymal subtypes based on their consensus signatures (11). In agreement with Fig. 1A, there was up-regulation (1.89-fold change) of SPCA2 (Fig. 1B) and conversely, down-regulation (0.61-fold change) of SPCA1 in epithelial-like breast cancer cell lines (Fig. 1C). To determine if these expression patterns extended to non-malignant mammary epithelial cells we examined cell density related changes in gene expression in sparse and confluent cultures of MCF10A. Unlike cancer cells, sparsely seeded MCF10A cells ceased to proliferate upon reaching confluence (Fig. 1D), due to contact inhibition and mesenchymal to epithelial transition (MET). Within 5 days post-confluence, we observed up-regulation of SPCA2 by 5-fold in MCF10A cultures, whereas SPCA1 levels decreased by 2-fold (Fig. 1E). These changes preceded the so-called "cadherin switch" that accompanies MET, characterized by increase in E-cadherin expression and reciprocal decrease of N-cadherin occurring 7-days post-confluence (Fig. 1E). The distinctive transcriptional signature of Golgi calcium pumps suggests isoform-specific functional differences and may be useful in defining breast cancer subtypes.

Tumor EMT scores quantitatively capture the molecular features of cancer cells exhibited during EMT (12). Tumors with high EMT score have high potential for

invasion and metastasis. We analyzed 633 breast cancer samples from TCGA to probe the link between EMT score and SPCA2 gene expression (20). Using Z-score of ±0.5 as cut-off for SPCA2 expression, breast cancer samples were grouped into low, intermediate and high expression categories. Tumors with low SPCA2 expression had significantly higher EMT score than those with high SPCA2 expression (Fig. 1F; $p<0.001$). This correlation was remarkably similar in tumors sorted for E-cadherin expression (Fig. 1G; $p<0.001$). No such correlation was observed for SPCA1 (Fig. 1H). Taken together, the robust correlation in gene expression between SPCA2 and E-cadherin point to a potential EMT-related functional link in breast cancer cells.

Loss of SPCA2 impairs E-cadherin biogenesis

Targeted knockdown of SPCA2 in MCF7 cells did not alter E-cadherin mRNA (Fig. 2A). However, total E-cadherin protein levels were significantly reduced (53 ± 7.6% of control; $p < 0.05$; Fig. 2B-C). In contrast, there was no significant change in E-cadherin protein expression upon SPCA1 knockdown (Fig. S2A-C), as previously reported in keratinocytes (20). There was no reduction of epidermal growth factor receptor (EGFR), a surface protein not found at the adherens junction, or of zona occludens-1 (ZO-1), a tight junction protein, in shSPCA2-treated cells (Fig. S2 D-G), which is consistent with a selective defect in E-cadherin biogenesis. Diminished E-cadherin expression in SPCA2-depleted MCF7 cells was confirmed by quantitative immunofluorescence microscopy (Fig. 2 D-E), which also revealed the bulk of the E-cadherin signal to be within intracellular compartments. This was further confirmed by

treatment of non-permeabilized MCF7 cells with antibody directed against an external epitope of E-cadherin, revealing a significant reduction in its surface expression in SPCA2-depleted cells (Fig. 2 F-G). As expected, E-cadherin trafficking in SPCA2-depleted MCF7 cells was restored by transfection of a FLAG-tagged and shRNA-resistant construct, SPCA2R (Figure 2H-I).

Interaction of SPCA2 with E-cadherin is independent of Ca^{2+} pump activity

Within the secretory pathway, luminal Ca^{2+} is important for sorting and processing of trafficked proteins. Therefore, we asked if the Ca^{2+} pumping activity of SPCA2 was required for E-cadherin biogenesis. A conserved aspartate is required for formation of the phosphoenzyme intermediate in all P-type ATPases, including SPCA2. Previously, we showed that mutation of this aspartate in SPCA2 (D379N) inactivated Ca^{2+} transport activity without affecting protein expression and Golgi localization (13). Unexpectedly, mutant D379N also restored E-cadherin expression to wild-type SPCA2R levels in shSPCA2-treated MCF7 cells (Figure 2H-I). This was confirmed by flow cytometry analysis: both SPCA2R and D379N mutant increased E-cadherin expression in knockdown cells to similar levels relative to the empty vector control, as seen by similar forward scatter in the upper right quadrant and shift in the histogram of cell population (Figure S3A-B), and by the increased number of cells with high E-cadherin (Figure 2J). These observations were extended to MDA-MB-231, a cell line expressing low endogenous levels of E-cadherin and SPCA2. Ectopic, tetracycline-induced expression of E-cadherin in these cells was significantly enhanced by introduction of SPCA2R or the

D379N mutant, evidenced by confocal microscopy analysis (Figure S3C-D) and FACS analysis (Figure S3E). These data point to a non-canonical, Ca^{2+} pump-independent and post-translational role for SPCA2 in E-cadherin biogenesis.

To probe the underlying mechanism for the pump-independent role of SPCA2 in E-cadherin biogenesis, we assessed protein-protein interactions by co-immunoprecipitation. Following ectopic expression of FLAG-SPCA2 and E-cadherin in HEK293T cells, antibody directed against E-cadherin co-immunoprecipitated FLAG-SPCA2 from cell lysates (Fig. 3A). Reciprocal immunoprecipitation of SPCA2 using the anti-FLAG antibody revealed bound E-cadherin by Western blotting, confirming protein interaction (Fig. 3A). Similar protein interaction was observed between E-cadherin and mutant D379N (Fig. 3B), consistent with the pump-independent function of SPCA2 in E-cadherin biogenesis. These findings suggest a chaperone-like role for SPCA2 to selectively regulate the trafficking and delivery of E-cadherin that could be critical to establish and maintain epithelial phenotypes.

Cell adhesion in tumorspheres requires SPCA2

The ability to form free-floating spheroids, known as tumorspheres or mammospheres, in suspension culture is broadly used to test cancer stem cell (CSC) activity (Fig. 3C) and has been shown to depend on surface expression of E-cadherin (21, 22). Knockdown of E-cadherin in MCF7 prevented tumorsphere formation, and conversely, over-expression of E-cadherin in non-spherogenic SKBR3 cells resulted in

sphere formation (21). Here, we evaluate tumorsphere formation in MCF7 cells that were treated with shRNA constructs to silence SPCA1 or SPCA2 expression as a proxy for E-cadherin mediated cell adhesion. Depletion of SPCA2 resulted in nearly complete loss of tumorspheres, with significant decrease in both number and size relative to scrambled shRNA control (Fig. 3D-E). In contrast, SPCA1 knockdown had no significant effect on tumorsphere formation (Fig. 3E). Following SPCA2 knockdown, both SPCA2R and the D379N mutant restored the ability to form tumorspheres (Fig. 3F-G), pointing to a pump-independent SPCA2 function required for cell adhesion.

SPCA2 is an upstream activator of Hippo signaling and EMT antagonist

Cell-adhesion mediated signaling pathways are important in contact inhibition of proliferation (23). Recently, E-cadherin was shown to activate the Hippo tumor suppressor signaling pathway to control phosphorylation and inactivation of YAP, resulting in nuclear exclusion and inhibition of cell proliferation in normal human mammary epithelial and breast cancer cells (Fig. 4A) (5, 7). Furthermore, a proteomic analysis of MCF7 cells showed that E-cadherin knockdown resulted in elevated expression of SLUG and ZEB1, downstream of YAP (24). Given the early post-confluency induction of SPCA2 gene expression ahead of the cadherin switch (Fig. 1E), together with the requirement for SPCA2 in E-cadherin biogenesis (Fig. 2), we postulated that SPCA2 may act upstream of E-cadherin to control subcellular localization of YAP. To test this hypothesis, MCF7 cells were cultured under sparse and confluent conditions and immunostained for YAP localization. As previously described for control cells,

nuclear occupancy of YAP in sparsely growing cells largely reverted to the cytoplasm upon reaching confluency (Fig. 4B, top panel) (5). In contrast, in cells depleted of SPCA2, YAP remained predominantly in the nucleus under both sparse and confluent culture conditions (Fig. 4B, bottom panel; Fig. 4C-E).

In the absence of SPCA2, nuclear YAP is expected to interact with the TEAD family of transcriptional activators to induce the expression of proliferative and anti-apoptotic genes that promote EMT and malignant transformation. Interestingly, expression of YAP, and the related co-activator TAZ, was negatively correlated with SPCA2 expression in patient breast cancer tissue from all cancer subtypes (7) (Fig. S4 A-B; $p = 3.23 \times 10^{-7}$, n = 295). Specifically, high YAP/TAZ expression is correlated with SPCA2 down-regulation in basal-like breast cancer (Fig. S4A). No correlation was observed between YAP/TAZ expression and that of SPCA1 (Fig. S4A, C; $p = 0.178$, n = 295). Therefore, down-regulation of SPCA2 may be permissive and prerequisite for EMT in breast cancer cells. To evaluate this possibility, we elicited EMT in MCF7 cells by treatment with EGF. Although SPCA1 transcript levels remained unchanged, SPCA2 levels decreased substantially upon EGF treatment (Fig. 4F). Consistent with induction of EMT, cells treated with EGF showed enhanced expression of EMT-associated genes including ZEB1, N-cadherin, SLUG/SNAI2 and Fibronectin (Fig. 4G-J, blue bars). For each of these genes, loss of SPCA2 was sufficient to elicit transcriptional induction even in the absence of EGF, and a further elevation of transcript was observed upon EGF treatment (Fig. 4G-J; gray bars). SPCA2 depletion also induced Vimentin transcription in MCF7 cells despite lack of effect of EGF treatment (Fig. 4K). Thus, SPCA2 maintains

antagonistic Hippo signaling for nuclear exclusion of YAP in confluent cells and suppression of downstream EMT associated genes.

DISCUSSION

Moonlighting proteins perform autonomous, mechanistically unrelated functions that serve an important role in linking different pathways (25). Here we show a Ca^{2+} transport-independent role for SPCA2 in E-cadherin biogenesis and formation of the adherens junction that expands its functional repertoire beyond an apparent functional redundancy with the ubiquitously expressed, housekeeping isoform SPCA1. Duplication of the SPCA gene occurred during tetrapod evolution (26) and paved the way for acquisition of novel functions. For example, the C-terminal tail of SPCA2 binds and activates store-independent Ca^{2+} influx through Orai1 to promote cell proliferation (13, 27). The selective chaperoning role of SPCA2 may stabilize E-cadherin levels in the Golgi although additional studies are needed for a detailed mechanism. Interestingly, loss of one functional copy of SPCA1 results in the ulcerative skin disorder, Hailey-Hailey disease arising from defective desmosomal adhesion in epidermal cells, although the underlying mechanism is unclear (28). Our findings may provide impetus for a more careful study of the biogenesis of desmosomal cadherins (desmoglein and desmocollin) in Hailey-Hailey disease.

Given the developmental and pathological implications of the EMT program, intensive efforts have been directed toward understanding the underlying molecular

mechanisms and regulatory networks. Down-regulation of E-cadherin is a defining mechanism in EMT. Most studies in the literature have focused primarily on silencing mutations in E-cadherin and transcriptional repression (3). However, a significant percentage of invasive tumors have normal E-cadherin gene and transcription, which may point to post-translational down-regulation of E-cadherin, although much less is known about these mechanisms (29). Intriguingly, dysregulation of membrane trafficking of E-cadherin has been implicated in EMT associated with viral oncogenesis, such as Rous sarcoma and Kaposi's sarcoma (30, 31). The post-translational, SPCA2-mediated regulation of E-cadherin trafficking we describe here provides new insights on mechanisms that regulate adherens junction stability in non-viral oncogenesis.

Down-regulation of SPCA2 is associated with basal and claudin-low breast cancer subtypes (15) that are characterized by hormone receptor negativity, a high degree of invasion and metastasis. Therefore, low SPCA2 may be a useful prognostic marker of the malignant invasive phenotype. Here, we demonstrate a causal link between SPCA2 down-regulation and induction of EMT. In contrast, high SPCA2 is characteristic of luminal A/B and HER2+ subtypes where it contributes to the formation of breast microcalcifications associated with tumorigenesis (15). We propose a model to summarize the role of SPCA2 in breast cancer. During the early stages of breast oncogenesis, proliferation and dysplasia of epithelial cells results in carcinoma *in situ*. Tumor cells in this stage express high levels of SPCA2, elevated cytoplasmic Ca^{2+} and rapid cell proliferation (13). Biogenesis and trafficking of E-cadherin is normal, cell-cell contacts are maintained and EMT genes are repressed. Induction of EMT in a subset of

breast cancer cells is associated with down-regulation of SPCA2 and other ESG, resulting in disrupted E-cadherin trafficking and enhanced EMT gene expression that facilitates intravasation of tumor cells and escape into the blood stream. Subsequently, extravasation of a subset of these breast cancer cells from the blood stream into tissues could be accompanied by mesenchymal to epithelial transition (MET) that reinstates expression of SPCA2 and other epithelial genes such as E-cadherin (32), resulting in secondary tumors at metastatic sites. Thus, the dysregulation of SPCA2 in breast cancer cells has novel clinical and pathological relevance resulting from distinct, subtype-specific roles in both oncogenesis and tumor suppression.

Author Contributions

D.D., J.P.L, H.P. and M.R.M. designed and performed the experiments, analyzed data and edited the manuscript. R.R. designed experiments and wrote the paper.

Acknowledgements

This work was supported by grants from the National Institutes of Health (GM62142 and DK103078) to R.R. H.P. was a Fulbright Fellow supported by the International Fulbright Science and Technology Award, and J.P. was supported in part by the PREP scholar program at Johns Hopkins.

REFERENCES

1. Kalluri R & Weinberg RA (2009) The basics of epithelial-mesenchymal transition. *The Journal of clinical investigation* 119(6):1420-1428.
2. Vega S, *et al.* (2004) Snail blocks the cell cycle and confers resistance to cell death. *Genes Dev* 18(10):1131-1143.
3. Ashaie MA & Chowdhury EH (2016) Cadherins: The Superfamily Critically Involved in Breast Cancer. *Curr Pharm Des* 22(5):616-638.
4. Kovacs EM, Ali RG, McCormack AJ, & Yap AS (2002) E-cadherin homophilic ligation directly signals through Rac and phosphatidylinositol 3-kinase to regulate adhesive contacts. *The Journal of biological chemistry* 277(8):6708-6718.
5. Kim NG, Koh E, Chen X, & Gumbiner BM (2011) E-cadherin mediates contact inhibition of proliferation through Hippo signaling-pathway components. *Proceedings of the National Academy of Sciences of the United States of America* 108(29):11930-11935.
6. Gumbiner BM (2005) Regulation of cadherin-mediated adhesion in morphogenesis. *Nature reviews. Molecular cell biology* 6(8):622-634.
7. Gumbiner BM & Kim NG (2014) The Hippo-YAP signaling pathway and contact inhibition of growth. *Journal of cell science* 127(Pt 4):709-717.
8. Janse van Rensburg HJ & Yang X (2016) The roles of the Hippo pathway in cancer metastasis. *Cell Signal* 28(11):1761-1772.
9. Dubois C, *et al.* (2014) Remodeling of channel-forming ORAI proteins determines an oncogenic switch in prostate cancer. *Cancer Cell* 26(1):19-32.
10. Janda E, *et al.* (2006) Raf plus TGFbeta-dependent EMT is initiated by endocytosis and lysosomal degradation of E-cadherin. *Oncogene* 25(54):7117-7130.
11. Kohn KW, Zeeberg BM, Reinhold WC, & Pommier Y (2014) Gene expression correlations in human cancer cell lines define molecular interaction networks for epithelial phenotype. *PLoS One* 9(6):e99269.
12. Tan TZ, *et al.* (2014) Epithelial-mesenchymal transition spectrum quantification and its efficacy in deciphering survival and drug responses of cancer patients. *EMBO Mol Med* 6(10):1279-1293.
13. Feng M, *et al.* (2010) Store-independent activation of Orai1 by SPCA2 in mammary tumors. *Cell* 143(1):84-98.
14. Grice DM, *et al.* (2010) Golgi calcium pump secretory pathway calcium ATPase 1 (SPCA1) is a key regulator of insulin-like growth factor receptor (IGF1R) processing in the basal-like breast cancer cell line MDA-MB-231. *The Journal of biological chemistry* 285(48):37458-37466.
15. Dang D, Prasad H, & Rao R (2017) Secretory pathway Ca(2+) -ATPases promote in vitro microcalcifications in breast cancer cells. *Mol Carcinog* 56(11):2474-2485.
16. Xiang M, Mohamalawari D, & Rao R (2005) A novel isoform of the secretory pathway Ca2+,Mn(2+)-ATPase, hSPCA2, has unusual properties and is expressed in the brain. *The Journal of biological chemistry* 280(12):11608-11614.

17. Vanoevelen J, *et al.* (2005) The secretory pathway Ca2+/Mn2+-ATPase 2 is a Golgi-localized pump with high affinity for Ca2+ ions. *The Journal of biological chemistry* 280(24):22800-22808.
18. Pollack JR, *et al.* (2002) Microarray analysis reveals a major direct role of DNA copy number alteration in the transcriptional program of human breast tumors. *Proceedings of the National Academy of Sciences of the United States of America* 99(20):12963-12968.
19. Sun Q, *et al.* (2012) Covariation of copy number located at 16q22.1: new evidence in mammary ductal carcinoma. *Oncology reports* 28(6):2156-2162.
20. Raiko L, *et al.* (2012) Hailey-Hailey disease and tight junctions: Claudins 1 and 4 are regulated by ATP2C1 gene encoding Ca(2+) /Mn(2+) ATPase SPCA1 in cultured keratinocytes. *Exp Dermatol* 21(8):586-591.
21. Manuel Iglesias J, *et al.* (2013) Mammosphere Formation in Breast Carcinoma Cell Lines Depends upon Expression of E-cadherin. *PLoS One* 8(10):e77281.
22. Powan P, Luanpitpong S, He X, Rojanasakul Y, & Chanvorachote P (2017) Detachment-induced E-cadherin expression promotes 3D tumor spheroid formation but inhibits tumor formation and metastasis of lung cancer cells. *Am J Physiol Cell Physiol* 313(5):C556-C566.
23. Ozawa M (2015) The N-cadherin cytoplasmic domain confers anchorage-independent growth and the loss of contact inhibition. *Sci Rep* 5:15368.
24. Vergara D, *et al.* (2015) Proteomics analysis of E-cadherin knockdown in epithelial breast cancer cells. *J Biotechnol* 202:3-11.
25. Huberts DH & van der Klei IJ (2010) Moonlighting proteins: an intriguing mode of multitasking. *Biochimica et biophysica acta* 1803(4):520-525.
26. Pestov NB, *et al.* (2012) Structural evolution and tissue-specific expression of tetrapod-specific second isoform of secretory pathway Ca2+-ATPase. *Biochemical and biophysical research communications* 417(4):1298-1303.
27. Cross BM, Hack A, Reinhardt TA, & Rao R (2013) SPCA2 regulates Orai1 trafficking and store independent Ca2+ entry in a model of lactation. *PLoS One* 8(6):e67348.
28. Hu Z, *et al.* (2000) Mutations in ATP2C1, encoding a calcium pump, cause Hailey-Hailey disease. *Nat Genet* 24(1):61-65.
29. Thiery JP (2003) Epithelial-mesenchymal transitions in development and pathologies. *Curr Opin Cell Biol* 15(6):740-746.
30. Palacios F, Tushir JS, Fujita Y, & D'Souza-Schorey C (2005) Lysosomal targeting of E-cadherin: a unique mechanism for the down-regulation of cell-cell adhesion during epithelial to mesenchymal transitions. *Molecular and cellular biology* 25(1):389-402.
31. Qian LW, Greene W, Ye F, & Gao SJ (2008) Kaposi's sarcoma-associated herpesvirus disrupts adherens junctions and increases endothelial permeability by inducing degradation of VE-cadherin. *Journal of virology* 82(23):11902-11912.
32. Wells A, Yates C, & Shepard CR (2008) E-cadherin as an indicator of mesenchymal to epithelial reverting transitions during the metastatic seeding of disseminated carcinomas. *Clin Exp Metastasis* 25(6):621-628.

33. Cancer Genome Atlas N (2012) Comprehensive molecular portraits of human breast tumours. *Nature* 490(7418):61-70.
34. Barretina J, *et al.* (2012) The Cancer Cell Line Encyclopedia enables predictive modelling of anticancer drug sensitivity. *Nature* 483(7391):603-607.

Figure Legends

Figure 1. SPCA2 is an epithelial marker co-expressed with E-cadherin

(A) Hierarchical clustering and heat map of the correlation coefficient matrix of SPCA isoforms with ESG and MSG in breast cancer samples from TCGA (low correlation, blue; high correlation, red; n=526) (33). SPCA1 and SPCA2 cluster with MSG and ESG, respectively. Note the strong correlation of SPCA2 with *CDH1* (red asterisk). (B-C) Breast cancer cell lines from CCLE grouped as mesenchymal or epithelial to show Z-scores for SPCA2 (B) and SPCA1 (C) mRNA (11, 34). Note, significant up-regulation of SPCA2 and conversely, significant down-regulation of SPCA1 in epithelial-like breast cancer cell lines. ***$p<0.001$, Student's t-test. (D) MCF10A cells were cultured in both sparse and confluent conditions and DIC images were taken with 10X and 20X objectives on a Zeiss Axio Observer A.1 microscope. (E) qPCR analysis of SPCA2, SPCA1, E-cadherin and N-cadherin expression in cDNA extracted from sparse cells or after 5 or 7 days post-confluence. ***$p<0.001$, **$p<0.01$, two-tailed Welch's t-test, n=3. (F-H) Box and whisker with scatter plots of the EMT score across 633 breast cancer samples from the TCGA dataset grouped into low, intermediate and high expression categories for SPCA2 (F), E-cadherin (G) and SPCA1 (H) (***$p<0.001$) (20). Notably, tumors with low SPCA2 or E-cadherin expression had significantly higher EMT score than those with high SPCA2 expression. See SI Appendix, Fig. S1.

Figure 1.

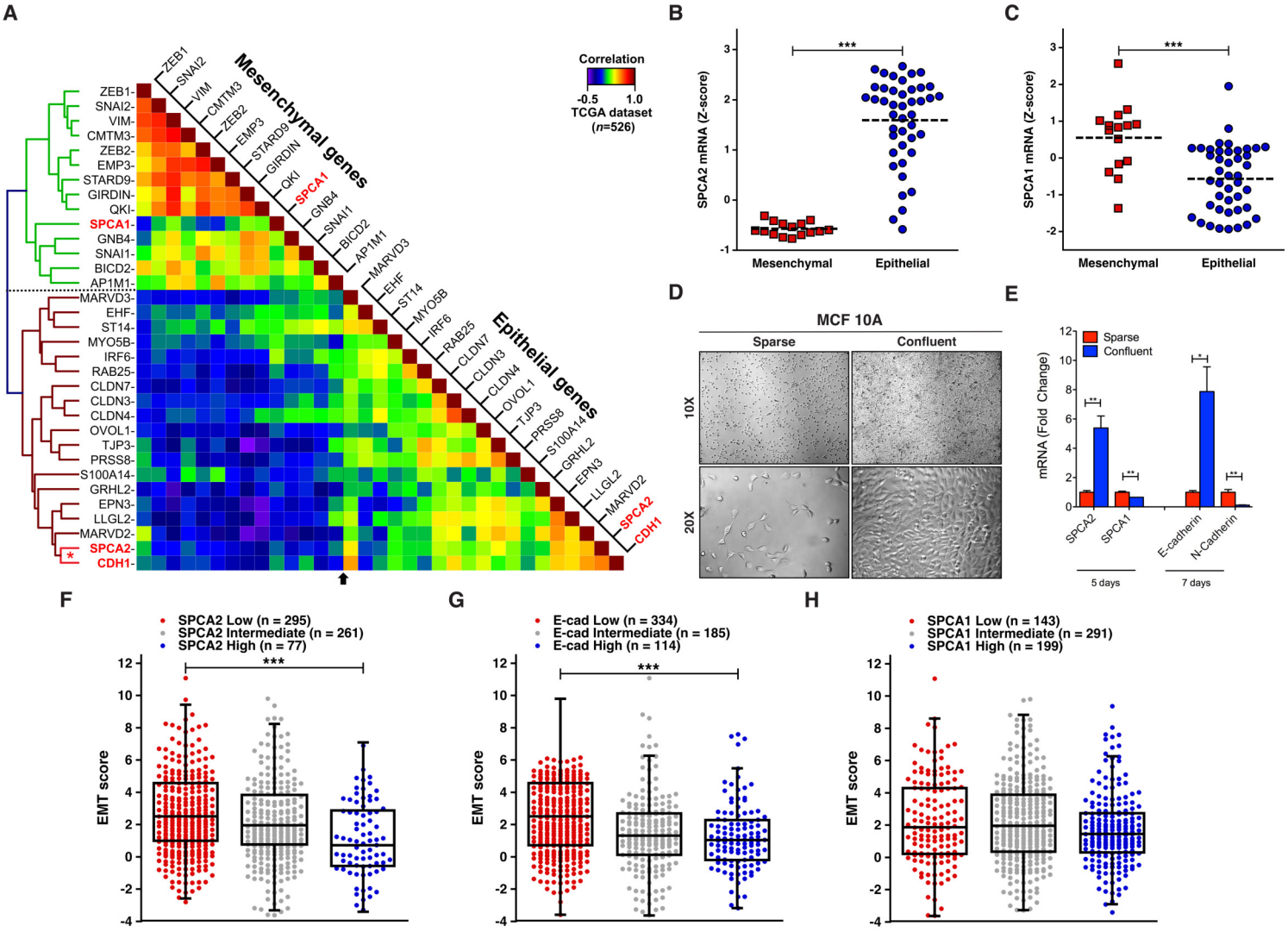
A
Mesenchymal genes
Epithelial genes
Correlation
-0.5
1.0
TCGA dataset
(n=526)
ZEB1
SNAI2
VIM
CMTM3
ZEB2
EMP3
STARD9
GIRDIN
QKI
SPCA1
GNB4
SNAI1
BICD2
AP1M1
MARVD3
EHF
ST14
MYO5B
IRF6
RAB25
CLDN7
CLDN3
CLDN4
OVOL1
TJP3
PRSS8
S100A14
GRHL2
EPN3
LLGL2
MARVD2
SPCA2
CDH1
B
SPCA2 mRNA (Z-score)
Mesenchymal
Epithelial
C
SPCA1 mRNA (Z-score)
Mesenchymal
Epithelial
D
MCF 10A
Sparse
Confluent
10X
20X
E
Sparse
Confluent
mRNA (Fold Change)
SPCA2
SPCA1
E-cadherin
N-Cadherin
5 days
7 days
F
SPCA2 Low (n = 295)
SPCA2 Intermediate (n = 261)
SPCA2 High (n = 77)
EMT score
G
E-cad Low (n = 334)
E-cad Intermediate (n = 185)
E-cad High (n = 114)
EMT score
H
SPCA1 Low (n = 143)
SPCA1 Intermediate (n = 291)
SPCA1 High (n = 199)
EMT score

Figure 2. Loss of SPCA2 impairs E-cadherin biogenesis

(A) Knockdown of SPCA2 in MCF7 cells was confirmed by qPCR. There was no change in E-cadherin transcript. **$p<0.01$, Student's t-test. (B) Western blot of cell lysates probed with antibody against E-cadherin and β-Actin. (C) E-cadherin protein expression from densitometric analysis of Western blots, normalized against β-Actin. *$p<0.05$, Student's t-test, n=3. (D) Immunofluorescence of E-cadherin in permeabilized MCF7 cells treated with both control and shSPCA2. Note that the antibody recognizes a cytoplasmic epitope (E) Total mean fluorescence from (D) was quantified. ***$p<0.001$, Student's t-test, control n=91, shSPCA2 n=44. (F) Immunofluorescence of surface E-cadherin in non-permeabilized MCF7 cells treated with both control and shSPCA2. Note that the antibody recognizes an extracellular epitope. (G) Total mean fluorescence was quantified. *$p<0.05$, Student's t-test, control n=276, shSPCA2 n=47. (H) Immunofluorescence of total E-cadherin in permeabilized MCF7 shSPCA2 cells expressing vector control, FLAG-tagged SPCA2R (Wild Type), or FLAG-tagged SPCA2 D379N mutant, with quantification (I). *$p<0.05$, **$p<0.01$, Student's t-test, vector n=34, SPCA2R n=44, D379N n=18. Scale bars are 20 μm. (J) Flow cytometry analysis of MCF7 shSPCA2 cells transfected with empty vector, SPCA2R, or D379N showing number of cells with high E-cadherin fluorescence (from Fig. S3A, pink shaded area). *$p<0.05$, ***$p<0.001$, Student's t-test, n=3 for each condition. See SI Appendix, Fig. S2 and S3.

Figure 2.

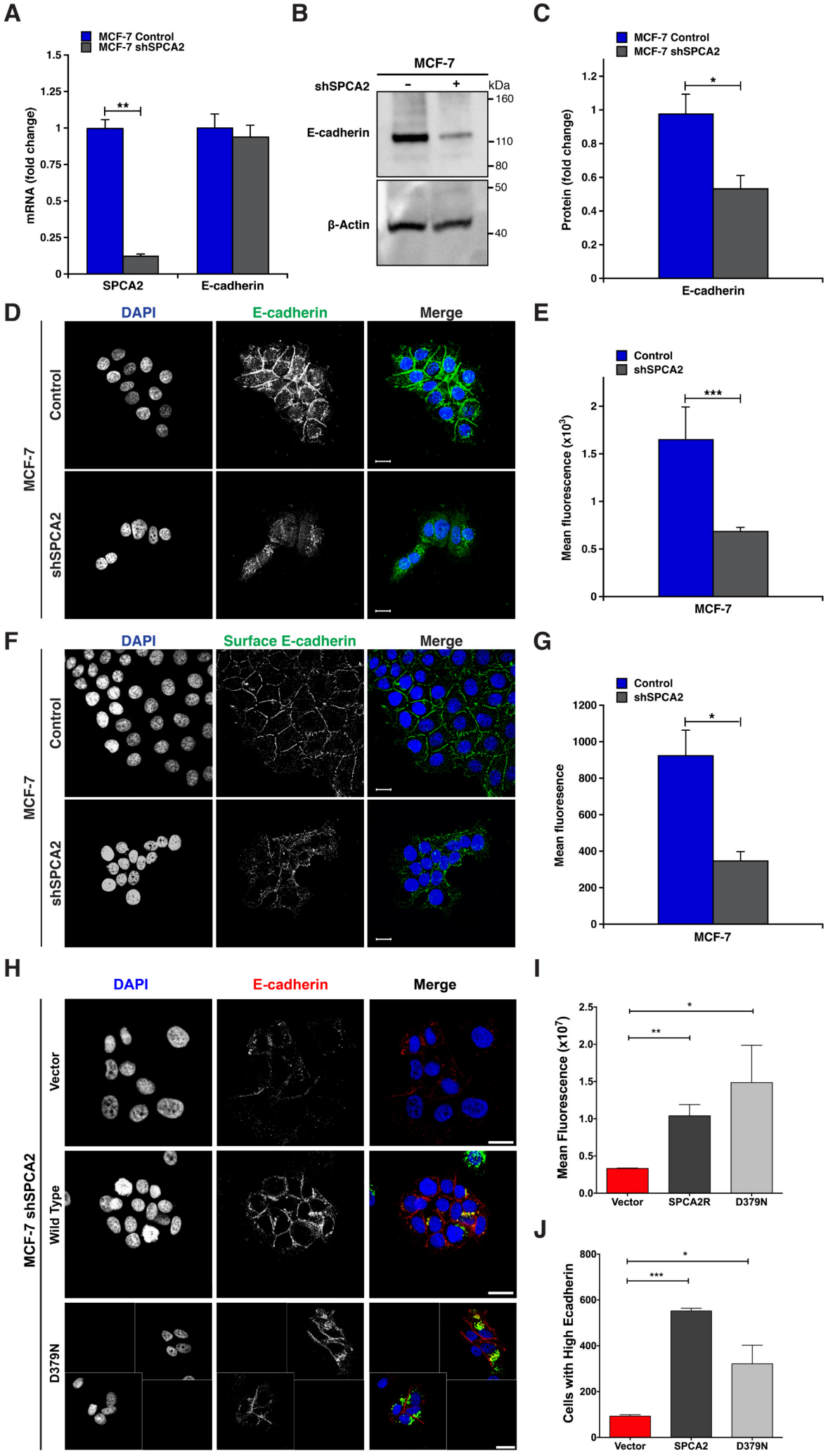
A
MCF-7 Control
MCF-7 shSPCA2
mRNA (fold change)
1.5
1.25
1
0.75
0.5
0.25
0
**
SPCA2
E-cadherin
B
MCF-7
shSPCA2
-
+
kDa
E-cadherin
β-Actin
160
110
80
50
40
C
MCF-7 Control
MCF-7 shSPCA2
Protein (fold change)
1.2
1
0.8
0.6
0.4
0.2
0
*
E-cadherin
D
DAPI
E-cadherin
Merge
MCF-7
Control
shSPCA2
E
Control
shSPCA2
Mean fluorescence (x10³)
2
1.5
1
0.5
0
***
MCF-7
F
DAPI
Surface E-cadherin
Merge
MCF-7
Control
shSPCA2
G
Control
shSPCA2
Mean fluoresence
1200
1000
800
600
400
200
0
*
MCF-7
H
DAPI
E-cadherin
Merge
MCF-7 shSPCA2
Vector
Wild Type
D379N
I
Mean Fluorescence (x10⁷)
2.5
2.0
1.5
1.0
0.5
0.0
*
**
Vector
SPCA2R
D379N
J
Cells with High Ecadherin
800
600
400
200
0
*
***
Vector
SPCA2
D379N

Figure 3. SPCA2 is required for tumorsphere formation

(A) Co-immunopreciptation of FLAG-SPCA2R and E-cadherin from HEK293T cells. Lanes indicate control antibody (IgG), cell lysate (Input), antibody to SPCA2 epitope (FLAG) or E-cadherin (E-cad). Blots were probed with antibody to E-cadherin, stripped and re-probed with FLAG antibody. (B) Co-immunoprecipitation of FLAG-D379N and E-cadherin from HEK293T cells. Lanes and western blots as in (A). (C) Schematic of MCF7 tumorsphere culture. (D-E) MCF-7 cells treated with scramble (control), shSPCA1 or shSPCA2 constructs were cultured to form tumorspheres. (D) Representative images of control and shSPCA2 cells are shown respectively in the upper and lower panels. (E) The numbers of tumorspheres (upper panel) and their diameters (lower panel) were quantified. **$p<0.01$, ***$p<0.001$, Student's t-test, n=3. (F) Three representative images of MCF7 shSPCA2 cells rescued with empty vector, SPCA2R, or SPCA2 D379N and cultured as tumorspheres. Scale bars are 50μm. (G) Tumorsphere area (upper panel) and number (lower panel) were quantified. ***$p<0.001$, Student's t-test; for tumorsphere area, n=31 for vector, n=45 for SPCA2R, and n=51 for D379N; for tumorsphere number per well, n=3 biological replicates for vector, SPCA2R, and D379N (not statistically significant). See SI Appendix.

Figure 3.

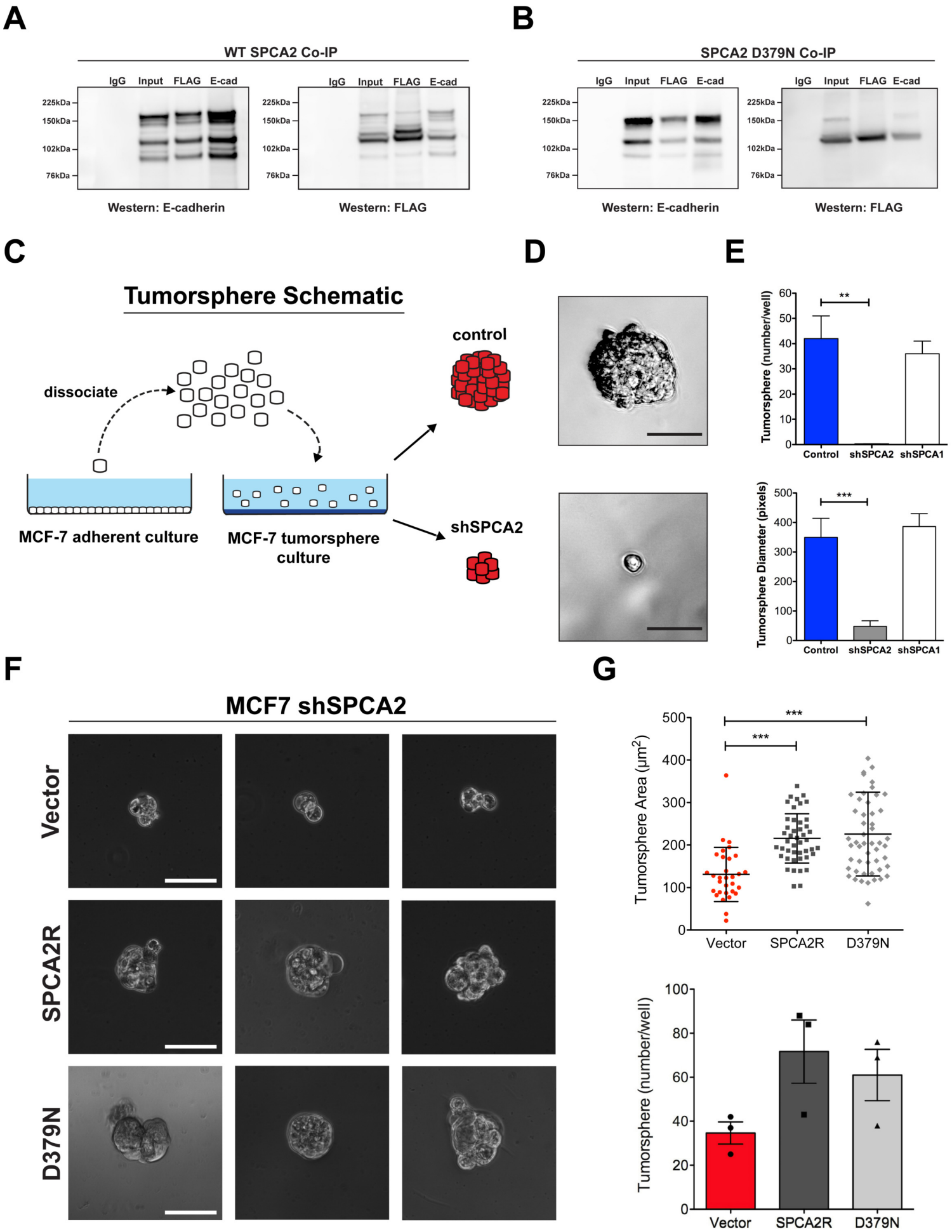
A
WT SPCA2 Co-IP
IgG Input FLAG E-cad
225kDa
150kDa
102kDa
76kDa
Western: E-cadherin
Western: FLAG
B
SPCA2 D379N Co-IP
Western: E-cadherin
Western: FLAG
C
Tumorsphere Schematic
dissociate
control
shSPCA2
MCF-7 adherent culture
MCF-7 tumorsphere culture
D
E
Tumorsphere (number/well)
Tumorsphere Diameter (pixels)
Control
shSPCA2
shSPCA1
F
MCF7 shSPCA2
Vector
SPCA2R
D379N
G
Tumorsphere Area (μm²)
Tumorsphere (number/well)
Vector
SPCA2R
D379N

Figure 4. SPCA2 controls YAP localization and its downstream EMT targets

(A) Schematic showing the role of Hippo-YAP signaling in control of EMT. Cell-cell contacts mediated by E-cadherin maintain nuclear exclusion of YAP, suppressing expression of EMT genes. (B) Immunofluorescence staining of YAP in MCF7 cells treated with scramble (control) or shSPCA2 and cultured under sparse or confluent conditions. Note the distribution of YAP localization between nuclei (stained with DAPI, blue) and cytoplasm. (C) Subcellular YAP distribution in MCF7 cells grown to confluence and stained as in (B). (D) Colocalization of YAP with DAPI staining in confluent MCF7 cells using Manders' coefficient. **$p<0.01$, Student's t-test. (E) Schematic of YAP localization in response to cell density, EGF treatment and SPCA2 knockdown. (F) Effect of EGF (20 ng/ml) on mRNA levels of SPCA1 and SPCA2 in MCF7 cells determined by qPCR. *$p<0.05$, Student's t-test. (G – K) MCF7 cells (control or SPCA2 knockdown) were treated with 20 ng/ml EGF and transcript levels of the following genes were determined by qPCR: Zeb1 (G), N-cadherin (H), SNAI2 (I), fibronectin (J), and vimentin (K). *$p<0.05$, **$p<0.01$, Student's t-test. See SI Appendix, Fig. S4.

Figure 4.

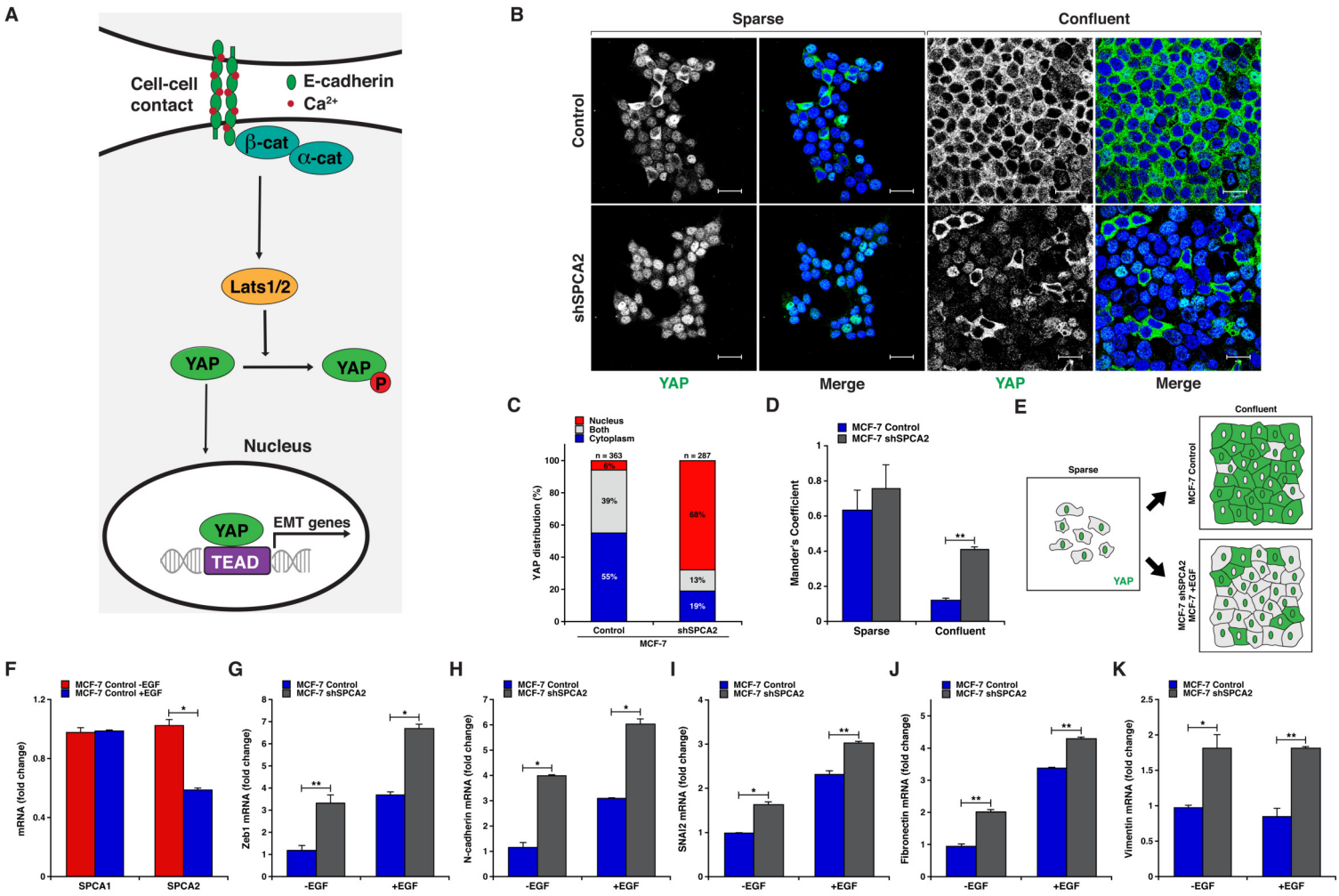
A
Cell-cell contact
E-cadherin
Ca2+
β-cat
α-cat
Lats1/2
YAP
YAP
P
Nucleus
YAP
EMT genes
TEAD
B
Sparse
Confluent
Control
shSPCA2
YAP
Merge
YAP
Merge
C
Nucleus
Both
Cytoplasm
n = 363
n = 287
6%
39%
55%
68%
13%
19%
YAP distribution (%)
Control
shSPCA2
MCF-7
D
MCF-7 Control
MCF-7 shSPCA2
Mander's Coefficient
Sparse
Confluent
E
Sparse
YAP
Confluent
MCF-7 Control
MCF-7 shSPCA2
MCF-7 +EGF
F
MCF-7 Control -EGF
MCF-7 Control +EGF
mRNA (fold change)
SPCA1
SPCA2
G
MCF-7 Control
MCF-7 shSPCA2
Zeb1 mRNA (fold change)
-EGF
+EGF
H
MCF-7 Control
MCF-7 shSPCA2
N-cadherin mRNA (fold change)
-EGF
+EGF
I
MCF-7 Control
MCF-7 shSPCA2
SNAI2 mRNA (fold change)
-EGF
+EGF
J
MCF-7 Control
MCF-7 shSPCA2
Fibronectin mRNA (fold change)
-EGF
+EGF
K
MCF-7 Control
MCF-7 shSPCA2
Vimentin mRNA (fold change)
-EGF
+EGF

A Moonlighting Role for SPCA2 in E-cadherin Biogenesis and Suppression of Epithelial-Mesenchymal Transition
Dang et al., 2018

Supplemental Experimental Procedures and Figures S1 to S4

EXPERIMENTAL PROCEDURES

Hierarchical clustering

CCLE and TCGA invasive breast carcinoma project datasets were accessed through cBioPortal (http://www.cbioportal.org/) (1). Hierarchical clustering to analyze gene expression data was performed with statistiXL software and results were displayed as a dendrogram and correlation coefficient matrix heat map.

Cell Culture

Cells used in this study were HEK293T (ATCC CRL-3216), MCF7 (ATCC HTB-22), and MCF10A (ATCC CRL-10317). MDA-MB-231 tet-Ecad cells were a generous gift from the Barry Gumbiner, Seattle Children's Hospital (2). HEK293T cells were cultured in monolayer with DMEM containing sodium pyruvate, antibiotic, antimycotic, and 10% serum. MDA-MB-231 tet-Ecad and MCF7 cells were cultured in monolayer with DMEM containing antibiotic, antimycotic, and 10% serum. MCF10A monolayer cells were cultured in DMEM/F12 containing 5% horse serum, 20ng/ml EGF, 0.5mg/ml hydrocortisone, 100ng/ml cholera toxin, 10µg/ml insulin, and 1X penicillin/streptomycin. 50ng/ml of EGF (Sigma-Aldrich, cat#E9644) was added to the culture for 6 hours to induce EMT. Cells were cultured with 5% CO_2 and at 37°C in a humidified incubator.

Lentiviral Transfection

FUGW overexpression constructs and pLK0.1 shRNA and lentiviral construction of both SPCA isoforms was packaged and transfected according to previous methods using pCMV-Δ8.9 and PMDG at a ratio using 9:8:1 in HEK293T cells. Virus was collected after 48 hours and concentrated with Lenti-X Concentrator (Clontech, Cat#631231) (3). After 48 hours of transfection, cells were selected with puromycin at varying concentrations according to kill curves performed for each specific cell line (1 – 2.5 mg/mL). Experiments were performed within 5 passages to ensure maintained knockdown.

cDNA synthesis & Quantitative PCR

1µg of RNA was collected and used for cDNA synthesis (Applied Biosystems, cat#4387406). The qPCR mastermix was made with EagleTaq Universal Mastermix (Roche, cat#07260296190), Taqman probe (Applied Biosystems; GAPDH (Hs02758991_g1), SPCA2 (Hs00939492_m1), SPCA1 (Hs00995930_m1), E-cadherin (Hs01023894_m1), N-cadherin (Hs00983056_m1), Zeb1 (Hs00232783_m1), Snail1 (Hs00195591_m1), and Vimentin (Hs00958111_m1)), and 50ng of cDNA.

Co-immunoprecipitation

Cell lysates were collected in NP-40 lysis buffer and quantified using the Pierce BCA Assay Kit (Thermo Scientific, cat#23225). 150µg of the lysate was resuspended in 150µl of lysis buffer for each antibody. For each co-IP, 30µl of Dynabeads magnetic protein G beads (Thermo Scientific, cat#10003D) were mixed with resuspended lysates on a rotating rack for 30 minutes at 4°C. Pre-cleared lysates were incubated with 1.5µg of the following antibodies on a rotating rack overnight at 4°C: IgG control (Cell Signaling Technology, cat#5415S), E-cadherin (BD Transduction Laboratories, cat#sc10804), FLAG (Sigma, cat#F1804), and V5 (Thermo Scientific, cat#R906-25). The antibody-lysate mixture was then incubated on a rotating rack for 4 hours at 4°C with 30µl of magnetic beads. Flow through was collected and saved and the beads were washed 2 times with PBS 0.01% tween buffer before eluting in 17µl 50mM glycine (pH 2.8). 6.25µl of NuPAGE LDS sample buffer (Thermo Fisher Scientific, cat#NP0007) and 2.5µl of NuPAGE sample reducing agent (Thermo Fisher Scientific, cat#NP0004) were added to the eluate. Samples were prepared and run on an SDS-PAGE protein gel and transferred to a membrane for Western blotting analysis.

Western Blotting
35 – 50μg of lysates were utilized for protein analysis. GAPDH (Sigma-Aldrich, cat#G9295) was used as the loading control for Western blotting. E-cadherin (BD Transduction Laboratories, cat#610181), ZO-1 (H-300) (Santa Cruz Biotechnology, cat#sc-10804), and EGFR antibody (Abcam, cat# ab2430) was analyzed for total protein. Blots were analyzed using ImageJ.

Immunofluorescence
Cells were cultured on glass coverslips and were rinsed with PBS and pre-extracted with 1X PHEM buffer, 8% sucrose and 0.025% saponin. Cells were fixed with 4% paraformaldehyde for 30 minutes and were rinsed and washed with PBS 3 times for 5 minutes each. After blocking in 1% BSA, cells were incubated with primary antibody overnight in 4°C. Cells were rinsed with 0.2% BSA 3 times for 5 minutes and were then incubated with a fluorescent secondary antibody in 1% BSA and 0.025% saponin buffer for 30 minutes at room temperature. Coverslips were washed and mounted onto slides with mounting media (Dako, cat#S3023). Immunofluorescent staining was analyzed using ImageJ. Antibodies and fluorescent probes are specified in Supplemental Experimental Procedures.

Tumorsphere Suspension Assay
MCF7 cells (1000 cells) were seeded and cultured and in serum free suspension media (DMEM, 31% L-glutamine, 1% penicillin/streptomycin, 2% B27 Supplement, 20ng/ml EGF, and 20ng/ml FGFb) in 6-well culture plates according to the method from Iglesias et al. (4). Culture plates were treated with poly (2-hydroxethyl methacrylate) (Sigma-Aldrich, cat# P3932) prior to culturing to prevent adherence. Tumorspheres were counted and measured using ImageJ.

YAP Localization
MCF-7 cells were infected with scramble "Control" or 'shSPCA2' lentivirus for 48 hrs, and then selected with puromycin (2.5 μg/mL) for 48 hrs. Following, cells were seeded either sparse or confluent on coverslips, as previously described (5). Briefly, adherent cells were serum starved for 24 h before fixation and subsequent immunofluorescence. MCF7 cells, due to an aberrant mutation in PI3-K that alters YAP trafficking, were treated with wortmannin (10 μM) for 4 h to restore normal YAP trafficking prior to fixation (5). YAP intracellular localization was analyzed with anti-YAP antibody (63.7) (Santa Cruz Biotechnology, cat#SC-101199) using confocal microscopy.

SUPPLEMENTAL FIGURE LEGENDS

Figure S1. SPCA2 is transcriptionally linked with E-cadherin in breast cancer
(A) Chromosomal locations of genes for E-cadherin and SPCA2 (chromosome 16), and for SPCA1 (chromosome 3), indicated by red lines. (B) Correlation of E-cadherin and SPCA2 copy number variation in cancer cell lines. Pearson coefficient = 0.81, $p=9.99x10^{-124}$. (C) Correlation of E-cadherin and SPCA2 mRNA expression in cancer cell lines. Pearson coefficient = 0.44, $p=2.52x10^{-26}$. (D) Copy-number levels of SPCA1 and E-cadherin gene expression. p=0.004; Pearson coefficient = 0.13. (E) mRNA levels of SPCA1 and E-cadherin gene expression. p=0.82; Pearson coefficient = 0.01.

Figure S2. Selective effects of SPCA gene knockdown on protein expression
(A) MCF7 cells were treated with scramble (control) or shSPCA1 constructs. mRNA for SPCA1 and E-cadherin was determined by qPCR. **p<0.01, ***p<0.001; Student's t-test, n=3. (B and C) Western blotting of E-cadherin in lysates from MCF7 cells treated with control or shSPCA1; protein levels were normalized to β-Actin and quantified from three independent transfections. (D and E) Western blotting of EGF receptor in MCF7 cells treated with control or shSPCA2; protein levels were normalized to GAPDH and quantified from three independent transfections. (F and G) Western blotting of ZO-1 in MCF7 cells treated with control or shSPCA2; protein levels were normalized to GAPDH and quantified from three independent transfections.

Figure S3. Ectopic expression of SPCA2 or mutant D379N enhances E-cadherin expression
(A) FACS scatter plots of MCF7 shSPCA2 cells rescued with FLAG-SPCA2R or FLAG-D379N. Cells were probed with primary antibody against FLAG and incubated with an Alexa Fluor 643 secondary, as

well as E-cadherin-FITC conjugated primary antibody and processed by flow cytometry. Red boxes are gates for cells expressing high levels of E-cadherin represented in Figure 2J. (B) Representative histograms for each condition were plotted with their respective median fluorescence values. (C) MDA-MB-231 tet-Ecadherin cells expressing either empty vector, wild type SPCA2, or D379N and treated with 2μg/ml of doxycycline and imaged using confocal microscopy. (D) Normalized fluorescence values for each condition. **$p<0.01$, ***$p<0.001$, Student's t-test, vector n=3, SPCA2R n=3, D379N n=3.

Figure S4. Transcriptional links between EMT-associated genes and SPCA
(A) Expression heatmap of YAP, the related co-activator TAZ, SPCA1 and SPCA2 in patient breast cancer tissue obtained from the GSE31448 microarray dataset (6). Note the reciprocal expression of SPCA2 with YAP and TAZ, particularly in basal-like breast cancer. (B-C) Scatter plot of SPCA2 (B) and SPCA1 (C) expression against YAP/TAZ expression levels from all breast cancer subtypes (n=295). SPCA2, but not SPCA1, is negatively correlated with YAP/TAZ expression ($p=3.23X10^{-7}$).

Supplemental References

1. Cerami E*, et al.* (2012) The cBio cancer genomics portal: an open platform for exploring multidimensional cancer genomics data. *Cancer Discov* 2(5):401-404.
2. Kim NG, Koh E, Chen X, & Gumbiner BM (2011) E-cadherin mediates contact inhibition of proliferation through Hippo signaling-pathway components. *Proceedings of the National Academy of Sciences of the United States of America* 108(29):11930-11935.
3. Feng M*, et al.* (2010) Store-independent activation of Orai1 by SPCA2 in mammary tumors. *Cell* 143(1):84-98.
4. Manuel Iglesias J*, et al.* (2013) Mammosphere Formation in Breast Carcinoma Cell Lines Depends upon Expression of E-cadherin. *PLoS One* 8(10):e77281.
5. Sun Y*, et al.* (2015) Stromal interaction molecule 1 (STIM1) silencing inhibits tumor growth and promotes cell cycle arrest and apoptosis in hypopharyngeal carcinoma. *Med Oncol* 32(5):150.
6. Sabatier R*, et al.* (2011) Down-regulation of ECRG4, a candidate tumor suppressor gene, in human breast cancer. *PLoS One* 6(11):e27656.

Figure S1.

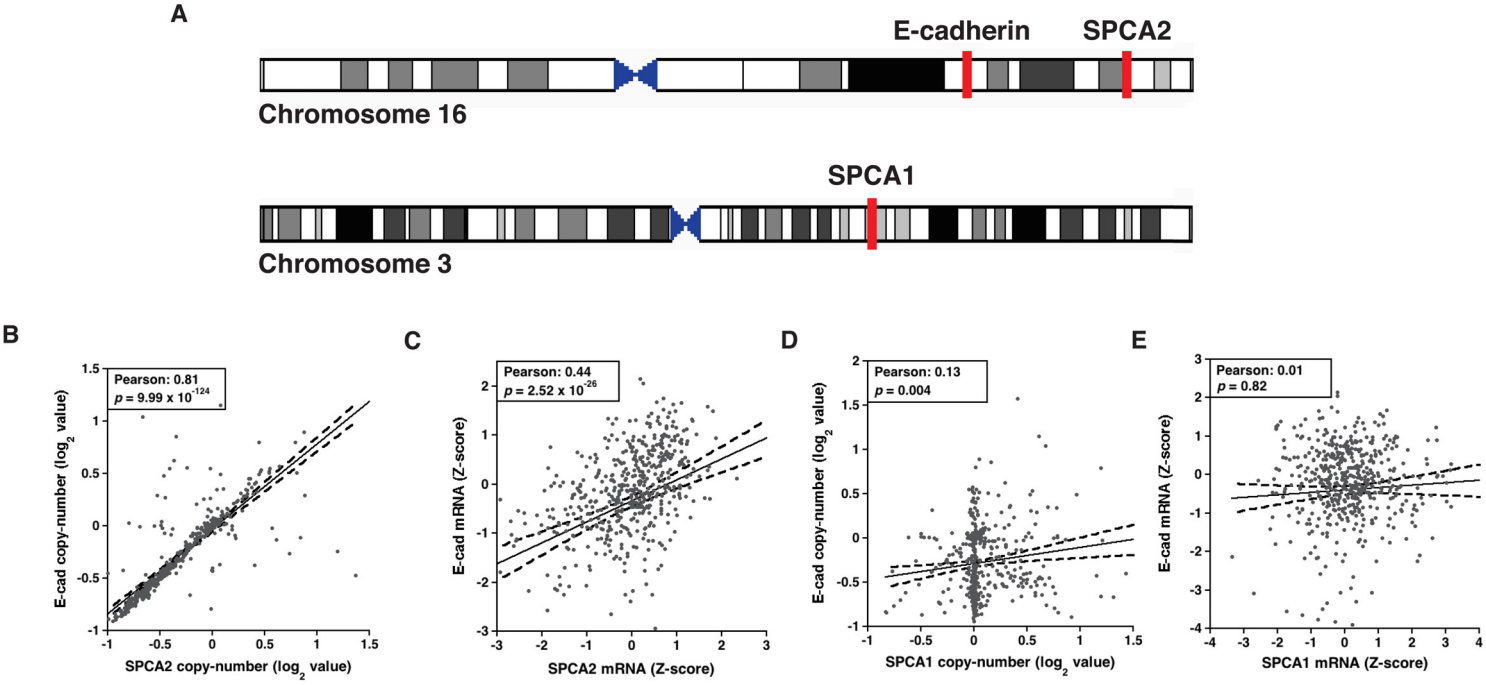
A
E-cadherin
SPCA2
Chromosome 16
SPCA1
Chromosome 3
B
Pearson: 0.81
p = 9.99 x 10^-124
E-cad copy-number (log2 value)
SPCA2 copy-number (log2 value)
C
Pearson: 0.44
p = 2.52 x 10^-26
E-cad mRNA (Z-score)
SPCA2 mRNA (Z-score)
D
Pearson: 0.13
p = 0.004
E-cad copy-number (log2 value)
SPCA1 copy-number (log2 value)
E
Pearson: 0.01
p = 0.82
E-cad mRNA (Z-score)
SPCA1 mRNA (Z-score)

Figure S2.

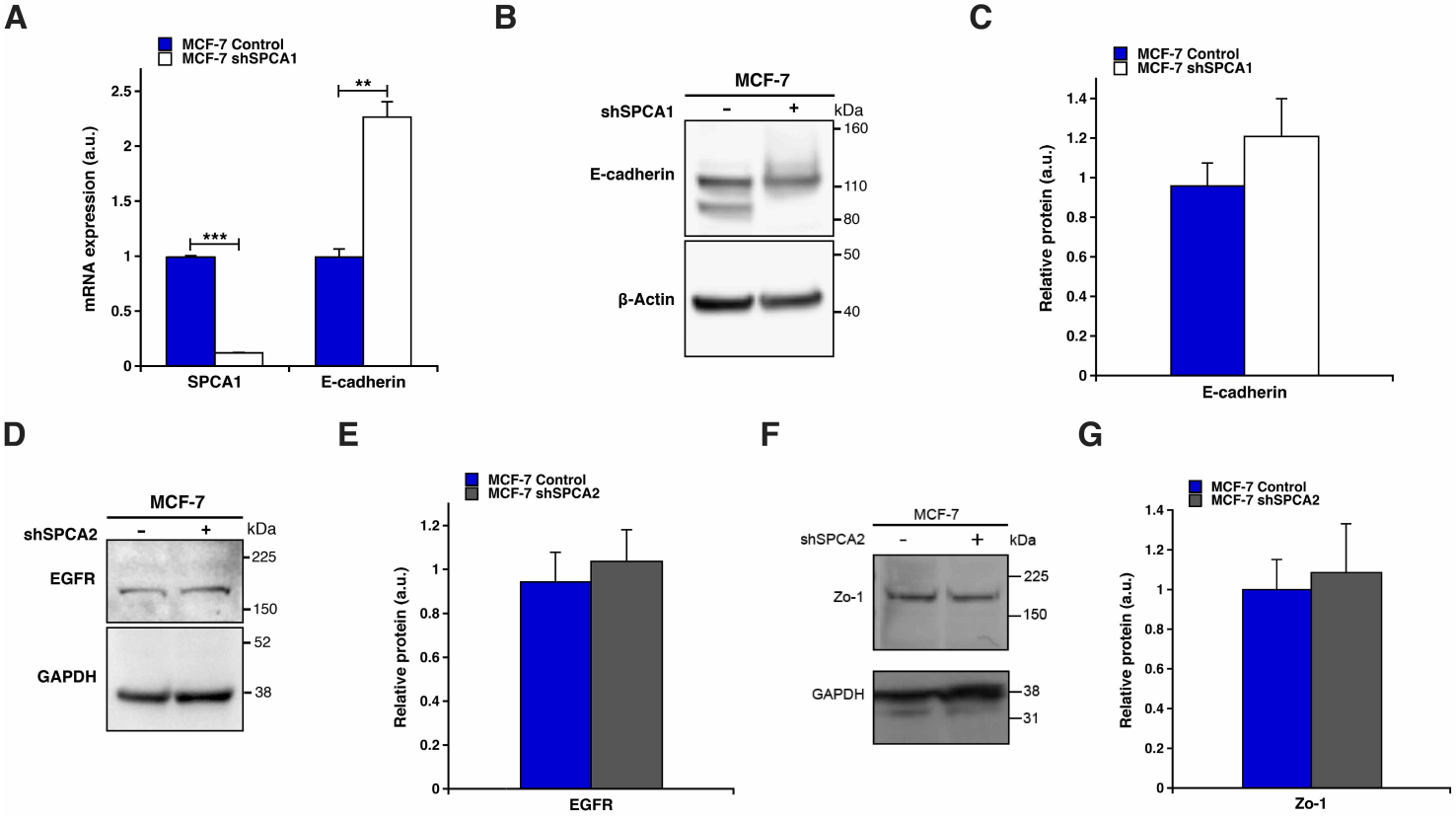
A
MCF-7 Control
MCF-7 shSPCA1
mRNA expression (a.u.)
2.5
2
1.5
1
0.5
0
***
**
SPCA1
E-cadherin
B
MCF-7
shSPCA1
-
+
kDa
E-cadherin
β-Actin
160
110
80
50
40
C
MCF-7 Control
MCF-7 shSPCA1
Relative protein (a.u.)
1.4
1.2
1
0.8
0.6
0.4
0.2
0
E-cadherin
D
MCF-7
shSPCA2
-
+
kDa
EGFR
GAPDH
225
150
52
38
E
MCF-7 Control
MCF-7 shSPCA2
Relative protein (a.u.)
1.2
1
0.8
0.6
0.4
0.2
0
EGFR
F
MCF-7
shSPCA2
-
+
kDa
Zo-1
GAPDH
225
150
38
31
G
MCF-7 Control
MCF-7 shSPCA2
Relative protein (a.u.)
1.4
1.2
1
0.8
0.6
0.4
0.2
0
Zo-1

Figure S3.

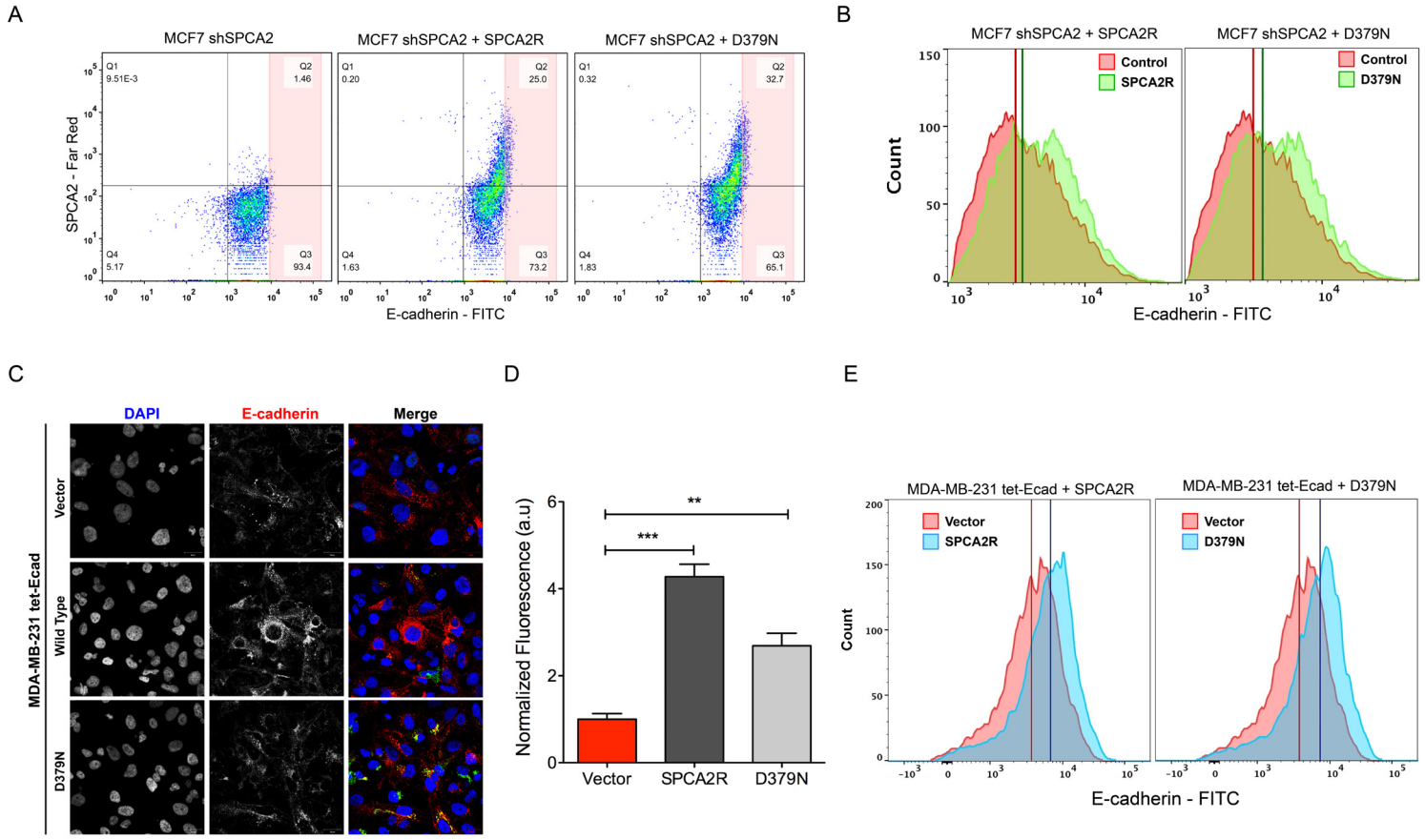
A
MCF7 shSPCA2
MCF7 shSPCA2 + SPCA2R
MCF7 shSPCA2 + D379N
SPCA2 - Far Red
E-cadherin - FITC
Q1 9.51E-3
Q2 1.46
Q4 5.17
Q3 93.4
Q1 0.20
Q2 25.0
Q4 1.63
Q3 73.2
Q1 0.32
Q2 32.7
Q4 1.83
Q3 65.1
B
MCF7 shSPCA2 + SPCA2R
MCF7 shSPCA2 + D379N
Control
SPCA2R
D379N
Count
E-cadherin - FITC
C
DAPI
E-cadherin
Merge
MDA-MB-231 tet-Ecad
Vector
Wild Type
D379N
D
Normalized Fluorescence (a.u)
**
***
Vector
SPCA2R
D379N
E
MDA-MB-231 tet-Ecad + SPCA2R
MDA-MB-231 tet-Ecad + D379N
Vector
SPCA2R
D379N
Count
E-cadherin - FITC

Figure S4.

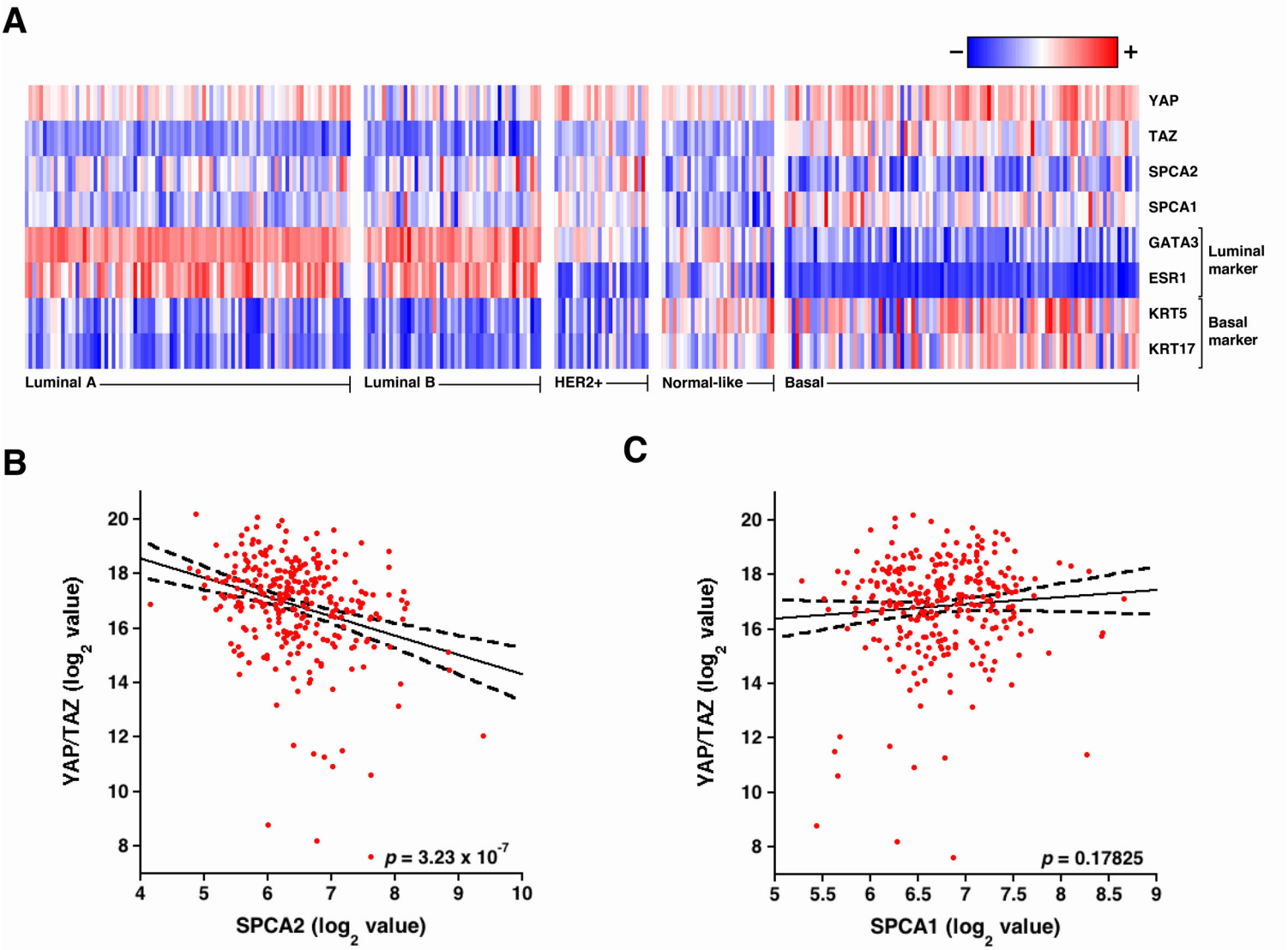
A
−
+
YAP
TAZ
SPCA2
SPCA1
GATA3
ESR1
Luminal marker
KRT5
KRT17
Basal marker
Luminal A
Luminal B
HER2+
Normal-like
Basal
B
YAP/TAZ (log2 value)
SPCA2 (log2 value)
p = 3.23 x 10-7
C
YAP/TAZ (log2 value)
SPCA1 (log2 value)
p = 0.17825